# Lattice Dynamics of Molybdenum at High Pressure

Daniel L. Farber,[1] Michael Krisch,[2] Daniele Antonangeli,[1,2] Alexandre Beraud,[2]
James Badro,[1,3] Florent Occelli,[1] and Daniel Orlikowski[4]

[1]*Earth Science Division, Lawrence Livermore National Laboratory, 7000 East Avenue, Livermore, California 94550, USA and Department of Earth Sciences, University of California, Santa Cruz, California 95064, USA*

[2]*European Synchrotron Radiation Facility, B.P. 220, F-38043 Grenoble Cedex, France*

[3]*Département de Minéralogie, Institut de Minéralogie et de Physique des Milieux Condensés, Institut de Physique du Globe de Paris, Université Paris, 75005 Paris, France*

[4]*Physics and Advanced Technology Directorate, Lawrence Livermore National Laboratory, 7000 East Avenue, Livermore, California 94550, USA*

(Received 25 October 2005; published 21 March 2006)

We have determined the lattice dynamics of molybdenum at high pressure to 37 GPa using high-resolution inelastic x-ray scattering. Over the investigated pressure range, we find a significant decrease in the $H$-point phonon anomaly. We also present calculations based on density functional theory that accurately predict this pressure dependence. Based on these results, we infer that the likely explanation for the $H$-point anomaly in molybdenum is strong electron-phonon coupling, which decreases upon compression due to the shift of the Fermi level with respect to the relevant electronic bands.

DOI: 10.1103/PhysRevLett.96.115502 PACS numbers: 63.20.Dj, 63.20.Kr, 71.15.Mb, 78.70.Ck

The physical properties of molybdenum are interesting in a number of aspects. In particular, its high-pressure behavior has received a lot of interest as Mo is one of the elements forming the basis of the ultrahigh-pressure scale and was used in the calibration of the ruby fluorescence pressure scale [1–3]. However, its static and dynamic equations of state are known to be in disagreement [4]. Thus, there have recently been studies probing the pressure dependence of the elastic tensor and high-pressure strength [5]. Furthermore, the 4$d$ transition elements display a rich variety of phonon dispersion effects that provide a fertile testing ground for modern theoretical descriptions of lattice dynamics [6]. Molybdenum, which is a bcc 4$d$ transition metal, has been the focus of numerous studies of electronic structure [7,8] and lattice dynamics [9–13]. While the theoretical treatments have to a great degree been successful at reproducing much of the experimental lattice dynamics observations, the large softening near the $H$ point has for the most part resisted first principles treatment. The phonons near the $H$ point have been well studied with neutron diffraction at 1 atm and room temperature [11,12] and also as a function of temperature to 1203 K [13]. With increasing temperature, the $H$-point phonon displays anomalous stiffening that has been proposed to arise from either intrinsic anharmonicity of the interatomic potential or electron-phonon coupling. To address the nature of these phonon anomalies, we have undertaken a high-pressure experimental study probing the lattice dynamics of molybdenum. In this regard, lattice compression provides a very convenient way to probe the interatomic potential, allowing one to study the nature of any anharmonic contributions, as well as electron-phonon interactions. However, until recently, the requirement of relatively large samples for neutron scattering experiments has, except in rare cases [14–16], limited the range of pressures over which direct lattice dynamical information could be gathered. With the advent of x-ray inelastic scattering techniques, these difficulties have to a great degree been overcome [17,18].

We conducted high-resolution inelastic x-ray scattering (IXS) experiments on beam line ID28 at the European Synchrotron Radiation Facility (ESRF) in Grenoble, France. The incident synchrotron radiation was monochromatized at 17.794 keV utilizing the Si(9 9 9) configuration. The scattered photons were energy analyzed by five crystal analyzers in Rowland circle geometry, giving a total instrumental energy resolution of 3 meV full width at half maximum (FWHM). The x-ray beam was focused by two mirrors in Kirkpatrick-Baez geometry to a spot of 25 $\mu$m horizontal $\times$ 60 $\mu$m vertical FWHM. The momentum transfer, given by $Q = 2k_0 \sin(\theta_s/2)$, where $k_0$ is the incident photon wave vector and $\theta_s$ the scattering angle, was selected by rotating the spectrometer arm in the horizontal plane about the sample position. All the spectra are collected in a constant $q$ mode (Fig. 1). The momentum resolution, set by slits in front of the analyzer crystals, was 0.3 nm$^{-1}$. The energy scans were performed by varying the monochromator temperature while the temperature of the analyzer was kept constant, according to the relation $\Delta E/E = \alpha \Delta T$, where $\alpha = 2.58 \times 10^{-6}$ K$^{-1}$ is the linear thermal expansion coefficient of Si at room temperature. Further details of the IXS instrumentation have been described elsewhere [19,20].

Our samples, which consisted of high-quality molybdenum single crystals, were cut with the surface normal parallel to the [110] direction. The small ($\sim$60 $\mu$m diameter by 20 $\mu$m thickness) single crystals were prepared in-house using femtosecond laser cutting and standard polish-

 

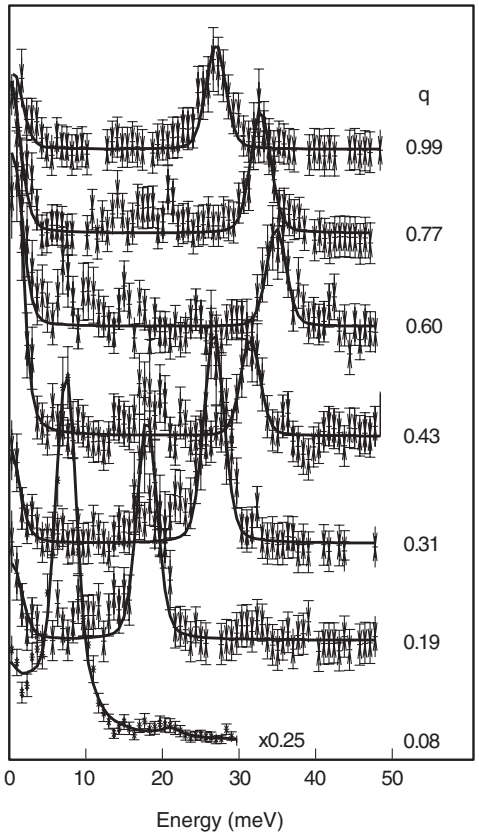


FIG. 1. Representative inelastic x-ray scattering data collected at 17 GPa. The data show the dispersion for the longitudinal acoustic mode along [001]. Note the softening in the spectra above $q = 0.6$.

ing techniques [21]. The crystals were loaded into diamond anvil cells (DAC), using helium as a pressure transmitting medium, to ensure hydrostatic pressure conditions and the preservation of the crystal quality during compression to high pressure. After preparation, the mosaic spreads (rocking curves) were better than 0.1 degrees, and throughout our experiments almost no sample degradation was observed, even for the highest pressure point. The pressure was determined by ruby fluorescence and cross-checked with the experimentally determined molybdenum hydrostatic equation of state [22].

We have used density functional theory (DFT) [23,24] to calculate the quasiharmonic phonon spectrum of molybdenum up to the highest experimental pressure of 37 GPa using linear response theory. The second derivatives of the total energy were calculated with respect to atomic displacements using a variational approach from which the dynamical matrix and phonon spectrum were calculated [25,26], using a plane-wave DFT code made possible through the ABINIT project [27,28].

The calculated phonon spectra are well converged with respect to several parameters. We used a norm-conserving Troullier-Martins [29] pseudopotential with six valence electrons ($4d^5 5s^1$) within the generalized gradient approximation (GGA) [30] for the exchange correlation function. The kinetic energy cutoff was determined to be 25 Hartree and a $24 \times 24 \times 24$ Monkhorst-Pack $k$-point grid [31] was found to yield convergence for the total energy. For the phonon spectrum, 29 irreducible $q$-points were used for the interpolation of the interatomic force constants. The total energies are converged to within $1 \times 10^{-16}$ Hartree for the ground state and $5 \times 10^{-7}$ Hartree for a given $q$ point. We have incorporated a standard Gaussian broadening scheme of the electron density of states to account for partially filled bands near the Fermi level ($\epsilon_F$) [32]. We found that the zone boundary phonons are quite sensitive to the broadening $\tau$, especially the $H$-point and $N$-point phonons, while this sensitivity is much less for the low $q$ phonons. After many tests, a broadening value $\tau = 0.01$ Ha was determined to give results for the entire calculated phonon spectrum most consistent with the experimental results [6] at ambient pressure (105.1 a.u.). Smaller broadening values yielded significantly lower phonon energies at the zone-edge, while higher values of $\tau$ nearly removed the $H$-point anomaly. The above numerical parameters were determined at ambient pressure, and subsequent calculations were performed at the experimentally determined volumes without any changes to these parameters. Overall, the calculated phonon dispersions compare very favorably with the experiment along the high symmetry directions and reproduce well both the known phonon anomalies ($H$-point and $2/3[111]$) at 1 bar [9] as well as the pressure evolution of these anomalies.

Previous interest in the theoretical treatment of the zone boundary modes near the $H$ point has been motivated by the observation of anomalous stiffening of the $H$-point phonon at ambient pressure with increasing temperature [13]. Although widely studied, progress on understanding the exact nature of this anomaly, and on improving theoretical descriptions of the phenomena, have to a great degree been hampered by a dearth of experimental data. All the proposed mechanisms are therefore in need of experimental verification. Though the $H$-point phonon is depressed by the well-known Kohn anomaly, arising from a strong decrease of the electronic screening [6], many theoretical descriptions have taken varying approaches. The effects of many-body renormalization of the electronic energies due to strong nesting of bands near $\epsilon_F$ have been considered [33], as well as intrinsic anharmonicity of the potential energy [34]. Furthermore, it has been pointed out that the ability to accurately reproduce the $H$-point anomaly critically hinges on the treatment of the $p$-like character of the bands near the Fermi surface, suggesting that anharmonic effects are negligible [35,36].

To address these issues, we have collected the phonon dispersions of all the branches at a pressure of 17 GPa (Fig. 2) and a partial set of dispersions (lacking only the transverse modes along [001] and [111]) at 37 GPa. These data represent the highest pressure set of dispersion curves

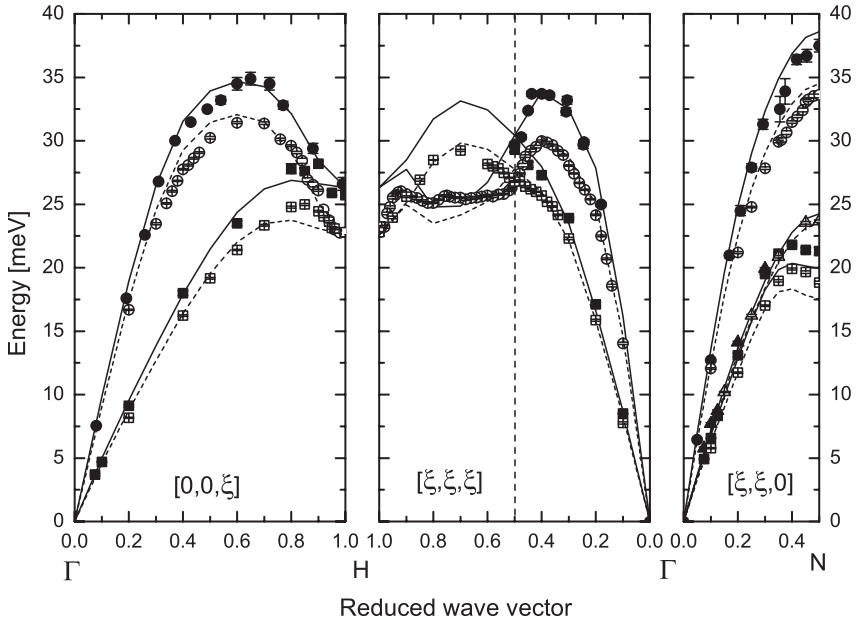


FIG. 2. Phonon dispersions in molybdenum. The filled symbols are IXS data collected at 17 GPa; the open symbols are inelastic neutron scattering results at 1 atm [9]. Circles are longitudinal acoustic modes; squares transverse acoustic modes. Along $[\xi\xi 0]$ the triangles and squares show the two nondegenerate transverse acoustic modes TA[110]⟨−110⟩ and TA[110]⟨001⟩, respectively. The dashed lines show the calculations performed at 105.1 a.u. (one atmosphere), and the solid lines the calculations at 99.2 a.u. (17 GPa).

yet reported for any material and clearly illustrate the power of the IXS technique for probing the dynamics of materials at high compressions. To check the consistency of our results with respect to ultrasonic measurements [37] we have also collected a set of low-$q$ spectra along [001] at 1 atm. Fits to the 1 atm IXS data compare with the ultrasonic measurements to better than ∼2% in $C_{44}$ and to better that 4% in $C_{11}$. Further, the agreement between our calculations and measured energies is quite good. Along Γ-$H$, the agreement in shape as well as absolute energies is very good, with exception of the TA branch where theory does not predict the overbending at about $q = 0.8$. Along Γ-$P$ the agreement is very good, aside from the TA branch from $q > 0.5$. However, along Γ-$N$, the experimental energies for the LA are consistently lower than the calculated values. Along this direction, the calculation of TA[110]⟨001⟩ while capturing the small softening near zone boundary is ∼5% low in energy. As shown in Fig. 3, our new high-pressure results show a profound decrease in the relative magnitude of the $H$-point phonon anomaly upon compression. This effect is highlighted in the inset, pointing up the differing density evolutions of the Grüneisen parameters at the maximum of the dispersion ($q \sim 0.65$) and at the $H$ point ($q = 1.0$). The rapid collapse of the $H$-point phonon anomaly in molybdenum is further illustrated by the comparison of the pressure dependence of the $H$-point mode measured in bcc-Fe. For similar volume compressions (5% in the case of Fe and 6% in the case of Mo) we find a ∼6% and ∼22% increase in the zone boundary mode in Fe and Mo, respectively [16].

A number of lines of evidence indicate that the explanation for the rapid decrease in the anomaly with pressure is a decrease in the magnitude of electron-phonon coupling on compression. Our DFT calculations treat all the $p$-like bands as part of the ion core, and yet, they accurately predict the pressure evolution of the $H$-point anomaly, thus ruling out to a great degree a large role for the $p$-like bands. Furthermore, upon compression at room temperature, the thermal excitations are both minimal and decrease with increasing pressure. This, in light of the fact that the computational methods used here are within the quasiharmonic approximation, suggests that intrinsic anharmonic contributions are unlikely to be responsible for the anomaly. Instead, we argue that the nested bands 3 and 4 near the Fermi level $\epsilon_F$ (at 1 atm) give rise to

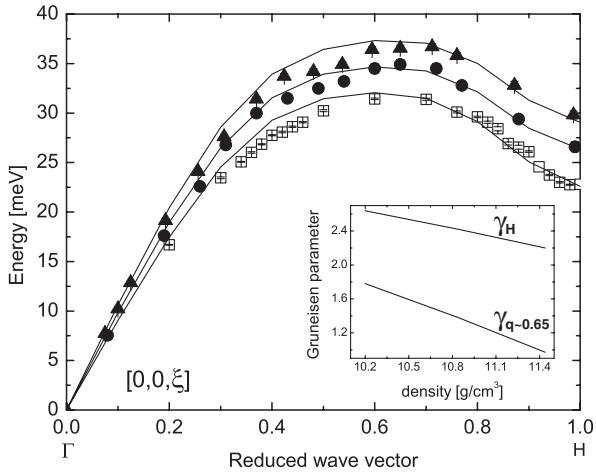


FIG. 3. Phonon dispersions along [001] as a function of pressure. Filled symbols are IXS data (circles, 17 GPa; triangles, 37 GPa); the unfilled squares are inelastic neutron scattering data (one atmosphere). Our calculations are shown as solid lines. The inset shows the Gruneisen parameter as a function of density for a $q \sim 0.65$, corresponding to the maximum in the dispersion, and at the $H$ point ($q = 1.0$).

the phonon anomaly. This conclusion is supported by our band structure calculations in two ways: (1) the first line of evidence for this reasoning comes from the sensitivity of the calculated $H$-point anomaly to Gaussian broadening $\tau$, which effectively broadens all the bands lessening any effect from nested bands 3 and 4, as mentioned above for the ambient pressure calculation, and vastly improving the agreement between the calculations and the experimental data at 1 atm; (2) as the system is compressed, band broadening also occurs but now solely due to the perturbation of the electronic structure in the compressed lattice. Furthermore, since the Fermi energy level increases under compression, at high pressure, the energy of the nested bands will be lower relative to $\epsilon_F$ (effectively moving outside of $k_BT$ from $\epsilon_F$). Therefore, both the pressure induced band broadening, and the lowering of nested bands relative to $\epsilon_F$, should favor a decrease in the $H$-point phonon anomaly, yielding a more ''normal'' bcc phonon spectrum, as experimentally observed. This sensitivity is to be expected if electron-phonon coupling is an important effect in the anomaly.

In conclusion, we have collected complete phonon dispersion curves at high pressures, to 37 GPa. From an experimental standpoint, the collection of lattice dynamical data at high-pressure is now mainly constrained by the strict requirements of sample quality, hydrostaticity, and diamond anvil cell technology, and no longer by the requirements of the probing technique itself. We have shown both experimentally and theoretically that the $H$-point anomaly on molybdenum rapidly decreases at pressures above $\sim$17 GPa. While not absolutely conclusive, based on our theoretical description of Mo, we argue that the most likely explanation for experimentally observed collapse of the $H$-point anomaly is a pressure induced decrease in the magnitude of electron-phonon coupling. Finally, we note that given the technical difficulty and expense of the experiments reported here, greatest potential to yield insight into complicated systems such as the 4$d$ transition metals, comes through a combined approach, where theoretical descriptions can both provide a fruitful subset of problems for focused high-pressure experiments and give insight into the nature of the underlying physics.

We thank J. A. Moriarty for helpful scientific discussions, C. Aracne, C. Boro, and D. Ruddle who all contributed critical efforts to the technical success of this project. M. Hanfland and D. Gibson for generous support with our samples and cells at the ESRF. This project was partially supported by the US NSF OISE 0340846. This work was performed under the auspices of the U.S. Department of Energy by University of California, Lawrence Livermore National Laboratory under Contract No. W-7405-Eng-48.

[1] A. B. Belonoshko *et al.*, Phys. Rev. Lett. **92**, 195701 (2004).
[2] D. Errandonea, Physica (Amsterdam) **B357**, 356 (2005).
[3] G. H. Miller, T. J. Ahrens, and E. M. Stolper, J. Appl. Phys. **63**, 4469 (1988).
[4] B. K. Godwal and R. Jeanloz, Phys. Rev. B **41**, 7440 (1990).
[5] T. S. Duffy *et al.*, J. Appl. Phys. **86**, 6729 (1999).
[6] C. M. Varma and W. Weber, Phys. Rev. Lett. **39**, 1094 (1977).
[7] D. D. Koelling *et al.*, Phys. Rev. B **10**, 4889 (1974).
[8] L. F. Mattheiss, Phys. Rev. **139**, A1893 (1965).
[9] B. M. Powell, P. Martel, and A. D. B. Woods, Phys. Rev. **171**, 727 (1968).
[10] C. B. Walker and P. A. Egelstaff, Phys. Rev. **177**, 1111 (1969).
[11] A. D. B. Woods and S. H. Chen, Solid State Commun. **2**, 233 (1964).
[12] A. D. B. Woods and B. M. Powell, Phys. Rev. Lett. **15**, 778 (1965).
[13] J. Zarestky *et al.*, Phys. Rev. B **28**, 697 (1983).
[14] T. Strassle *et al.*, Phys. Rev. Lett. **93**, 225901 (2004).
[15] S. Klotz, M. Braden, and J. M. Besson, Hyperfine Interact. **128**, 245 (2000).
[16] S. Klotz and M. Braden, Phys. Rev. Lett. **85**, 3209 (2000).
[17] F. Occelli, M. Krisch, P. Loubeyre, F. Sette, R. Le Toullec, C. Masciovecchio, and J. P. Rueff, Phys. Rev. B **63**, 224306 (2001).
[18] D. Antonangeli, M. Krisch, G. Fiquet, D. L. Farber, C. M. Aracne, J. Badro, F. Occelli, and H. Requardt, Phys. Rev. Lett. **93**, 215505 (2004).
[19] F. Sette, G. Ruocco, M. Krisch, C. Masciovecchio, and R. Verbeni, Phys. Scr. **T66**, 48 (1996).
[20] M. Krisch, J. Raman Spectrosc. **34**, 628 (2003).
[21] D. L. Farber, D. Antonangeli, C. M. Aracne, and J. Benterou, High Press. Res. (to be published).
[22] D. L. Farber *et al.* (unpublished).
[23] W. Kohn and L. J. Sham, Phys. Rev. **140**, A1133 (1965).
[24] P. Hohenberg and W. Kohn, Phys. Rev. **136**, B864 (1964).
[25] X. Gonze, Phys. Rev. B **55**, 10 337 (1997).
[26] X. Gonze, Phys. Rev. B **55**, 10 355 (1997).
[27] X. Gonze *et al.*, Comput. Mater. Sci. **25**, 478 (2002).
[28] S. Goedecker, SIAM J. Sci. Comput. **18**, 1605 (1997).
[29] N. Troullier and J. L. Martins, Phys. Rev. B **43**, 8861 (1991).
[30] J. P. Perdew and Y. Wang, Phys. Rev. B **45**, 13 244 (1992).
[31] H. J. Monkhorst and J. D. Pack, Phys. Rev. B **13**, 5188 (1976).
[32] C.-L. Fu and K.-M Ho, Phys. Rev. B **28**, 5480 (1983).
[33] C. L. Fu *et al.*, Phys. Rev. B **28**, 2957 (1983).
[34] Y. Wang *et al.*, J. Phys. Condens. Matter **14**, L453 (2002).
[35] S. Buck, K. Hummler, and M. Fahnle, Phys. Status Solidi B **195**, K9 (1996).
[36] D. Singh and H. Krakauer, Phys. Rev. B **43**, 1441 (1991).
[37] K. W. Katahara, M. H. Manghanani, and E. S. Fisher, J. Phys. F **9**, 773 (1979).